

# MAGNETOHYDRODYNAMIC EQUILIBRIUM AND STABILITY OF PRE-FLARE LOOPS

## *Constant Pitch Field*

S. S. HASAN

*Indian Institute of Astrophysics, Bangalore-560034, India*

(Received 26 January, 1979)

**Abstract.** The equilibrium and stability of a loop in which energy storage occurs prior to a solar flare is discussed. Working on the hypothesis, that the onset of the flare begins only after sufficient magnetic energy has been stored in the loop typical values of parameters which describe the equilibrium are found for a magnetic field with a constant twist. The stability of this configuration is examined next and it is shown that for the force-free case, the structure is always unstable to kinking for any degree of twist. However, a slight deviation from the force-free configuration, through the presence of a small positive transverse pressure gradient, can stabilize the loops for moderate degrees of twist. The range of wave-numbers for which instability occurs and the maximum growth rates are also presented. Lastly, it is shown that the pressure gradients required to stabilize a pre-flare loop do not lead to conflict with observations.

## 1. Introduction

Several recent observations, especially those carried out during the Skylab mission, have provided useful information about the flare configuration. It seems reasonably well established that the principal structure associated with a flare is a loop (Cheng and Widing, 1975; Kahler *et al.*, 1975; Pallavicini *et al.*, 1977). In this paper we shall examine the equilibrium and stability of a loop, using a somewhat idealized model for the magnetic field distribution within the loop. The consequence of introducing a small transverse pressure gradient on the stability of the loop will also be discussed.

Recently Van Hoven *et al.* (1977) (see also Giachetti *et al.*, 1977) have, in the context of coronal loops, studied the role of positive transverse pressure gradients on the MHD stability of a structure using a form for the magnetic field first suggested by Lundquist (1950). In this paper, we consider a different equilibrium configuration and, furthermore, solve the more general eigenvalue problem to determine the growth rates of the unstable modes rather than just the restricted problem of marginal stability.

## 2. General Considerations

Flare-loops have been studied extensively with good angular resolution (1" or about 700 km) in X-ray and EUV lines (Vorpal *et al.*, 1975; Cheng and Widing, 1975; Foukal, 1975). Owing to the high conductivity of the solar atmosphere, the magnetic field is effectively 'frozen' into the plasma, and therefore, the observed loops also outline magnetic structures. The loops are typically 2–7 Mm wide and 5–20 Mm high.

Their ends or 'feet' are usually anchored in the photosphere. Most of the information about flare loops comes from observations of small to medium flares, for which the dimensions mentioned above are typical. In this study we shall consider solely loops associated with such events, as detailed observations of large flares are still sparse.

There is evidence which suggests that loops exist prior to the onset of the flare on a time scale greater than a few hours (Petraso *et al.*, 1975; Brueckner, 1976). Since a flare involves the release of a large amount of energy (typically  $10^{21}$ – $10^{24}$  J), it seems natural to consider a pre-flare phase (PFP for short) of a loop, during which a gradual build-up of energy takes place. The mechanism for the build-up of the flare energy will be left unspecified, but it could possibly be along the lines suggested by Gold and Hoyle (1960), viz. through twists applied at the 'feet' of the loop by photospheric gas. These authors emphasize that the pre-flare build-up of energy must be a gradual one, for any sudden increase would lead to associated observable effects, contrary to the case. We exclude the possibility that the flare energy is derived solely from flux tubes which emerge from the photosphere just prior to the flare. Although there is some evidence for 'newly-emerging flux tubes', there are many examples of flares in which these were not observed.

We shall use the terms pre-flare loops and flare-loops to refer essentially to the same entity, henceforth referred to as just a loop, which is characterized by a PFP and a flare phase during which it roughly preserves its geometric identity. The magnetic field structure of loops is, unfortunately, not well known owing to the poor resolution of magnetic measurements in the corona. However, a feature of the magnetic field associated with flares which is generally accepted is that it is non-potential i.e. currents must be present (Rust and Bar, 1973; Altschuler, 1973). There is also some direct observational evidence to support this view (Severny, 1965; Moreton and Severny, 1968). We picture the PFP as one in which a build-up of current takes place starting from a configuration close to potential and proceeding till the current energy is roughly comparable to the flare energy. Furthermore, we postulate that during the PFP the configuration is MHD stable. This scenario is compatible with models of flares discussed by Gold and Hoyle (1960), Alfvén and Carlquist (1967), Hasan (1977), and Spicer (1976).

With this preamble, we shall now proceed with a quantitative analysis of the equilibrium and stability of a loop.

### 3. Basic Equations

We assume that the problem under study can be treated using the ideal equations of MHD. These are in MKS units (Krall and Trivelpiece, 1973):

$$\partial\rho/\partial t + \text{div}(\rho\mathbf{v}) = 0, \quad (3.1)$$

$$\rho \frac{d\mathbf{v}}{dt} = -\text{grad } p + \mathbf{j} \times \mathbf{B}, \quad (3.2)$$

$$\text{curl } \mathbf{B} = \mu_0 \mathbf{j}, \quad (3.3)$$

$$\text{curl } \mathbf{E} = -\partial \mathbf{B} / \partial t, \quad (3.4)$$

$$\text{div } \mathbf{B} = 0, \quad (3.5)$$

$$\mathbf{E} + \mathbf{V} \times \mathbf{B} = 0, \quad (3.6)$$

$$\frac{d}{dt}(p/\rho^\gamma) = 0. \quad (3.7)$$

The symbols  $\rho$ ,  $\mathbf{v}$ ,  $\mathbf{B}$ ,  $\mathbf{j}$ ,  $\mathbf{E}$ , and  $p$  refer to mass density, velocity, magnetic field, current density, electric field, and pressure, respectively. Equation (3.1) is the equation of continuity, (3.2) is the equation of motion, (3.3)–(3.5) are Maxwell's equations, (3.6) is Ohm's law for an infinitely conducting plasma, and (3.7) is the equation of state for an adiabatic gas where  $\gamma$  is the ratio of specific heats. The above equations have to be supplemented with suitable boundary conditions, which are for a plasma–plasma interface, assuming a weakly curved boundary (Krall and Trivelpiece, 1973):

$$[p + B^2/2\mu_0] = 0, \quad (3.8)$$

$$\hat{n} \cdot [\mathbf{B}] = 0, \quad (3.9)$$

$$\hat{n} \times [\mathbf{B}] = \mu_0 \mathbf{K}, \quad (3.10)$$

$$\hat{n} \cdot [\mathbf{v}] = 0, \quad (3.11)$$

$$\hat{n} \times [\mathbf{E}] = \hat{n} \times \mathbf{v} \times [\mathbf{B}], \quad (3.12)$$

where  $\mathbf{K}$  is the surface current density, the brackets denote the jump in the enclosed quantity across the boundary and  $\hat{n}$  is a unit vector normal to the boundary.

#### 4. Equilibrium State

Let the equilibrium configuration be one in which there is no electric field, no mass motion and the plasma density is uniform within the loop. The relevant equations which describe the equilibrium are:

$$-\text{grad } p + \mathbf{j} \times \mathbf{B} = 0, \quad (4.1)$$

$$\text{curl } \mathbf{B} = \mu_0 \mathbf{j}, \quad (4.2)$$

$$\text{div } \mathbf{B} = 0. \quad (4.3)$$

For mathematical simplification we assume that the loop is weakly curved, so that to a first approximation it can be essentially regarded as a cylinder. Thus if  $R$  and  $a$  denote the global and channel radii of the loop, then it is assumed that  $R/a \gg 1$ . We shall use cylindrical coordinates and furthermore, assume (a) cylindrical symmetry (b) zero radial component of the magnetic field (c) the field lines to have a constant pitch  $2\pi/\mu$  where  $\mu = B_z/rB_\theta$ .

Under these assumptions, (4.1) and (4.2) give ((4.3) is trivially satisfied)

$$\frac{d}{dr}(p + B^2/2\mu_0) = -B_\theta^2/\mu_0 r. \quad (4.4)$$

Using the condition that the pitch of the field is constant, (4.4) gives an equation which relates  $p$  to  $B_\theta$ . A possible equilibrium solution to (4.4) for  $r \leq a$  is (Goedbloed and Hagebuk, 1972)

$$B_z(r) = B_0/(1 + \varepsilon^2 r^2), \quad (4.5)$$

$$B_\theta(r) = B_0 \mu r / (1 + \varepsilon^2 r^2), \quad (4.6)$$

$$p(r) = p_0 + (B_0^2/2\mu_0) \frac{\varepsilon^2 - \mu^2}{\varepsilon^2} \left[ 1 - \frac{1}{(1 + \varepsilon^2 r^2)^2} \right]. \quad (4.7)$$

The subscript 0 denotes the value on the axis and  $\varepsilon$  is a constant. For  $\mu = \varepsilon$ , there is no pressure variation and we get the force-free field of Gold and Hoyle (1960).

We assume that the loop is surrounded by a homogeneous plasma which is current free. The equilibrium state for  $r > a$ , will be described by

$$B_{0e} = 0, \quad B_{ze} = B_z(a) \quad \text{and} \quad p_e = \text{constant}. \quad (4.8)$$

The equilibrium quantities given by (4.5)–(4.7) and (4.8) have to be matched by the boundary conditions (3.8)–(3.12).

Equation (3.8) which expresses continuity of the total pressure at  $r = a$ , gives

$$(1 + \varepsilon^2 a^2)^{-1} \beta_e = \beta_0 + \frac{\varepsilon^2 - \mu^2}{\varepsilon^2} \left[ 1 - \frac{1}{(1 + \varepsilon^2 a^2)^2} \right] + \frac{u^2 a^2}{(1 + \varepsilon^2 a^2)^2}, \quad (4.9)$$

where  $\beta = 2\mu_0 p / B^2$ .

Equation (3.9) is trivially satisfied. There is a current at the surface  $r = a$ , owing to the discontinuity of  $B_\theta$ . From (3.10), we find that the surface current density has a magnitude  $B_\theta(a)/\mu_0$  and is directed opposite to the main current flowing within the loop.

The energy in the axial current is given by

$$W = \int (B_\theta^2/2\mu_0) dV = \frac{F^2 L}{2\pi a^2 \mu_0} f(\mu, \varepsilon), \quad (4.10)$$

where the integral is over the volume of the loop,  $L$  is the length of the loop,

$$f(\mu, \varepsilon) = \frac{\mu^2 a^2}{\ln(1 + \varepsilon^2 a^2)} \left[ 1 - \frac{\varepsilon^2 a^2}{1 + \varepsilon^2 a^2} \frac{1}{\ln(1 + \varepsilon^2 a^2)} \right], \quad (4.11)$$

and  $F$  is the longitudinal magnetic flux within the loop given by

$$F = 2\pi \int_0^a B_z r dr = B_0 \pi a^2 \frac{\ln(1 + \varepsilon^2 a^2)}{\varepsilon^2 a^2}. \quad (4.12)$$

We can use (4.10) to find a plausible range for  $\mu$  and  $\varepsilon$  using typical values for  $W$ ,  $F$ ,  $L$ , and  $a$ . Thus

$$f(\mu, \varepsilon) = \frac{2\mu_0}{F^2} \left(\frac{a}{R}\right) a W_\theta,$$

where we have assumed  $R = L/\pi$ . Let us take  $a \approx 2000$  km,  $a/R \approx \frac{1}{8}$  and  $W \approx 10^{21}$  J which is the energy typical of a sub-flare. Since the magnetic flux is the same throughout the length of the loop, we can use observations of photospheric flux concentration (e.g. Livingston and Harvey, 1969; Harvey and Harvey, 1973) to consider an appropriate value for  $F$ . Taking  $F \approx 3 \times 10^{10}$  Weber which corresponds to an average longitudinal field of about  $0.0025$  Wb m<sup>-2</sup> we get

$$f(\mu, \varepsilon) \approx 1.$$

If the field is approximately force-free,  $\mu \approx \varepsilon$  and hence we get from (4.11)

$$\mu a \approx \varepsilon a \approx 1.5. \quad (4.13)$$

From (4.12), we can find the field on the axis of the loop for the parameters we have used. This gives

$$B_0 \approx 0.005 \text{ Wb m}^{-2}.$$

Incidentally, the current density and total current in the loop can also be determined. The axial current density is given by the expression

$$J_z = \frac{2F}{\mu_0 \pi} \frac{\mu \varepsilon^3}{(1 + \varepsilon^2 r^2) \ln(1 + \varepsilon^2 a^2)}.$$

For the values just used, the maximum value of the current density occurs at  $r = 0$ , and is for  $\mu a \approx \varepsilon a \approx 1.5$

$$J_z^{\max} \approx 5 \times 10^{-4} \text{ A m}^{-2}. \quad (4.14)$$

The total current in the loop is given by

$$I \approx 2 \times 10^{10} \text{ A}. \quad (4.15)$$

For given values of  $F$ ,  $a$ , and  $L$  we see from (4.10) that the energy is a function of  $\mu a$  and  $\varepsilon a$ . Figure 1 depicts the variation of  $f$  as a function of  $\mu a$ , for the force-free case. We see from (4.10) that the energy increases monotonically with  $\mu a$ . Thus during the PFP, the configuration evolves from a state characterized by  $\mu \approx 0$  (i.e. zero current) to one in which  $\mu$  is large enough so that there is adequate energy in the current for a flare. The value of  $\mu$  corresponding to some specific values of the energy can be determined from (4.10). We have seen that a typical final value for  $\mu a$  is about 1.5.

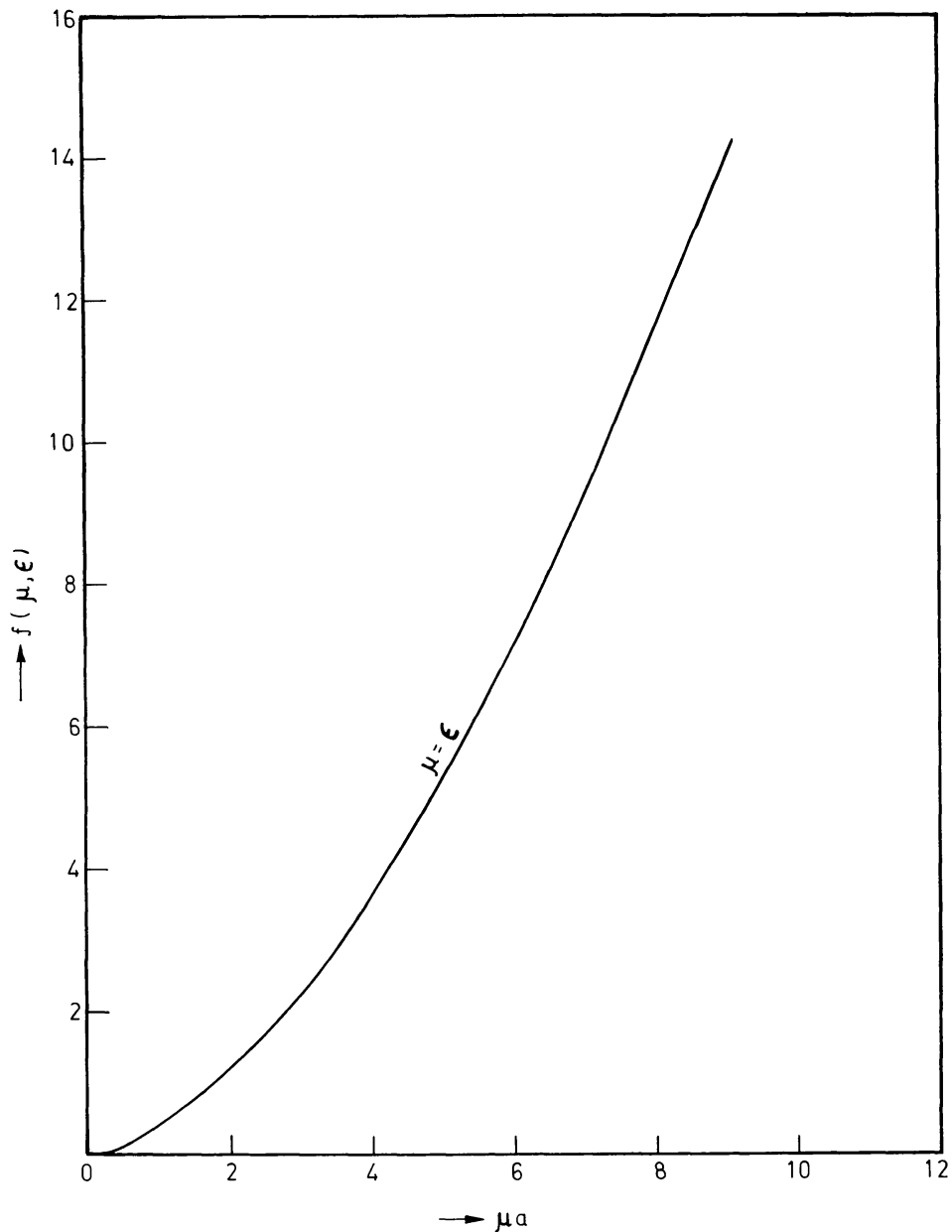


Fig. 1. The variation of  $f(\mu, \varepsilon)$  with  $\mu a$  is shown when the field is force-free.

### 5. MHD Stability

We shall study the stability of the equilibrium described in the previous section by examining its response to small perturbations. Let  $\xi$  denote a small displacement of a plasma element from its equilibrium position. Then it can be shown, to first order in  $\xi$ , that the system of equations (3.1)–(3.7) reduces to the following vector equation (Bernstein *et al.*, 1958)

$$\rho \frac{\partial^2 \xi}{\partial t^2} = \text{grad} (\gamma p \text{ div } \xi + \xi \cdot \text{grad } p) - \mu_0^{-1} \mathbf{Q} \times \text{curl } \mathbf{B} - \mu_0^{-1} \mathbf{B} \times \text{curl } \mathbf{Q}, \quad (5.1)$$

where

$$\mathbf{Q} = \text{curl} (\boldsymbol{\xi} \times \mathbf{B}).$$

We now look for normal modes of the system. Since the geometry is cylindrical, we choose the perturbations to be of the form  $\exp [i(kz + m\theta - \omega t)]$  multiplied by a quantity which is solely a function of  $r$ . The quantities  $k$ ,  $m$ , and  $\omega$  are constants, where  $m$  is an integer, which are characteristic of the normal mode. With this choice for  $\boldsymbol{\xi}$  we get from (5.1) the following equation for the radial component of the displacement, for  $r \leq a$  (Lust and Hain, 1957; Goedbloed and Hagebuk, 1972):

$$\frac{d}{dr} \left[ p(r) \frac{1}{r} \frac{d}{dr} (r\xi_r) \right] + q(r)\xi_r = 0, \quad (5.2)$$

where

$$\begin{aligned} p(r) &= (\omega^2 \rho - C^2/\mu_0) \{ \omega^2 \rho (\gamma p + B^2/\mu_0) - \gamma p C^2/\mu_0 \} N^{-1}, \\ q(r) &= (\omega^2 \rho - C^2/\mu_0) - 2 \frac{B_\theta}{\mu_0} \frac{d}{dr} \left( \frac{B_\theta}{r} \right) - \frac{4k^2 B_\theta^2}{\mu_0 r^2} \times \\ &\quad \times \left( \omega^2 \frac{\rho B^2}{\mu_0} - \gamma \frac{p C^2}{\mu_0} \right) N^{-1} + r \frac{d}{dr} \left\{ 2k B_\theta \left( \omega^2 \rho \left( \gamma p + \frac{B^2}{\mu_0} \right) - \gamma \frac{p C^2}{\mu_0} \right) \times \right. \\ &\quad \left. \times \left( \frac{m B_z}{r} - k B_\theta \right) N^{-1} \right\}, \end{aligned}$$

$$C = k B_z + m B_\theta / r,$$

$$N = \omega^4 \rho^2 - \omega^2 \rho (m^2/r^2 + k^2) (\gamma p + B^2 \mu_0) + (m^2/r^2 + k^2) \gamma p C^2 / \mu_0.$$

We shall look for solutions to (5.2) which are well behaved at  $r = 0$ . For  $r > a$ , we have

$$\frac{1}{r} \frac{d}{dr} \left( \rho \frac{d\xi}{dr} \right) - (\Lambda^2 + m^2/r^2) \xi = 0, \quad (5.3)$$

where

$$\xi = \frac{d\xi_{r,e}}{dr}, \quad \Lambda^2 = \frac{(\omega^2/s^2 - k^2)(\omega^2/h^2 - k^2)}{(\omega^2/s^2 + \omega^2/h^2 - k^2)},$$

$s = \sqrt{\gamma p_e / \rho_e}$  (sound speed) and  $h = B_e / \sqrt{\mu_0 \rho_e}$  (Alfvén speed). The solution of (5.3), which does not blow up at  $r = \infty$  is

$$\xi = A K_m(\Lambda r), \quad (5.4)$$

where  $K_m$  denotes a modified Bessel function of order  $m$  and  $A$  is a constant. The solutions of (5.2) and (5.3) have to be matched at  $r = a$ . Equation (3.12) can be integrated to yield the condition

$$\xi_r = A \Lambda K'_m(\Lambda a), \quad (5.5)$$

where the prime denotes differentiation with respect to the argument. Equation (3.8) gives the following equivalent condition:

$$\left[ -\gamma p \operatorname{div} \boldsymbol{\xi} + \mathbf{B} \cdot \mathbf{Q} / \mu_0 + \xi_n \frac{\partial}{\partial n} (B^2 / 2\mu_0) \right]_{r=a} = 0 \quad (5.6)$$

(where we have used (4.8) to eliminate the zero order quantities). Equations (5.6) and (5.5) give

$$f \xi_a - g/a \frac{d}{dr} (r \xi_a) |_{r=a} = d, \quad (5.7)$$

where

$$\begin{aligned} f &= 2k B_\theta (k B_\theta - m B_z / a) \times \\ &\quad \times [\omega^2 \rho (\gamma p + B^2 / \mu_0) - \gamma p C^2 / \mu_0] N^{-1} + B_\theta^2 / \mu_0 a, \\ g &= (\omega^2 \rho - C^2 / \mu_0) [\omega^2 \rho (\gamma p + B^2 / \mu_0) - \gamma p C^2 / \mu_0] N^{-1}, \\ d &= B_e^2 / \mu_0 (\omega^2 / h^2 - k^2) K_m(\Lambda a) / \Lambda a K'_m(\Lambda a). \end{aligned}$$

Equations (5.2) and (5.7) along with the requirement that  $r \xi_r = 0$  at  $r = 0$  constitute a generalized eigenvalue problem in  $\omega^2$ .

In the most general case, we shall attempt a numerical solution to the problem. However, in the limits  $\mu a \ll 1$ ,  $\varepsilon a \ll 1$  and  $ka \ll 1$  (5.2) is considerably simplified and an analytical solution is possible.

### 5.1. SMALL $M$

Let us define the following dimensionless variables:

$$\begin{aligned} \Omega^2 &= \omega^2 \rho \mu_0 a^2 / B_0^2, & u &= r/a, & B_0 &= 2\mu_0 p_0 / B_0^2, \\ K &= ka, & M &= \mu a, & E &= \varepsilon a \quad \text{and} \quad K_{\parallel} = K + mM. \end{aligned}$$

For  $m > 1$ , and using the approximations just mentioned (5.2) reduces to (Goedbloed and Hagebuk, 1972)

$$\frac{1}{u} \frac{d}{du} \left( u \frac{d\chi}{du} \right) + (b_m^2 - m^2 / u^2) \chi = 0, \quad (5.8)$$

where  $\chi = r \xi_r$ ,

$$\begin{aligned} b_m^2 &= \frac{m^2}{\Omega^2 - K_{\parallel}^2} \left[ \frac{4K^2 M^2}{m^2} \frac{\Omega^2 (\frac{1}{2} \gamma \beta)}{\Omega^2 (\frac{1}{2} \gamma \beta + 1) - \frac{1}{2} \gamma \beta K_{\parallel}^2} + 4M^2 \Pi - \right. \\ &\quad \left. - \frac{8M\Pi}{m} K_{\parallel} - \frac{4K^2 M}{m^3} K_{\parallel} - \frac{4M^2 K_{\parallel}^2}{m^2} \right], \end{aligned} \quad (5.9)$$

and  $\Pi = E^2 - M^2$ .

The solution of (5.8) which is finite at  $r = 0$  is

$$\chi = B J_m(b_m u), \quad (5.10)$$

where  $B$  is a constant and  $J_m$  denotes an ordinary Bessel function of order  $m$ .



From (5.7) and (5.10), we obtain the following dispersion relation:

$$\left\{ \frac{2KM}{m^2}(m - KM) + M^2 + Z^2 \frac{K_m(X)}{XK'_m(X)} \right\} \times \\ \times J_m(b_m) - (K_{\parallel}^2/m^2)b_m J'_m(b_m) = 0, \quad (5.11)$$

where

$$Z^2 = K^2 - \Omega^2 \rho_0 / \rho_e, \quad (5.12)$$

$$Y^2 = K^2 - \frac{\Omega^2}{(\frac{1}{2}\gamma\beta)} p_e / p_0, \quad (5.13)$$

$$X^2 = Z^2 Y^2 \left[ K^2 - \Omega^2 \rho_0 / \rho_e \left( 1 + \frac{1}{(\frac{1}{2}\gamma\beta)} p_e / p_0 \right) \right]^{-1}. \quad (5.14)$$

Instability occurs for  $K_{\parallel} = 0$  or  $K \simeq -mM$  (this will be borne out in the subsequent analysis). Thus (5.11) gives

$$\frac{J_m(b_m)}{b_m J'_m(b_m)} = \frac{K_{\parallel}^2}{m^2} \frac{1}{Z^2 G_m(X) - M^2}, \quad (5.15a)$$

where  $G_m(X) = K_m(X)/XK'_m(X)$ . For simplicity, we assume that the external medium is a vacuum. This involves no essential loss of generality in determining a criterion for instability. It can be seen from (5.12) and (5.13), that the wave-numbers corresponding to marginal stability are independent of the nature of the external medium. Thus (5.15a) simplifies to

$$\frac{J_m(b_m)}{b_m J'_m(b_m)} = -\frac{K_{\parallel}^2}{m^2 M^2} \frac{1}{m^2 + 1} \quad (5.15b)$$

as  $G_m(K) \simeq -1$  for  $K \ll 1$ .

As  $\Omega^2$  is purely real, the unstable modes correspond to  $\Omega^2 < 0$  (Bernstein *et al.*, 1958).

From (5.9), we can see that  $b_m$  decreases monotonically with increasing  $-\Omega^2$ . Therefore, the most rapidly growing modes are those for which (5.15b) is satisfied with the smallest value of  $b_m$ . Thus, we must have

$$j'_{m,1} < b_m \leq j_{m,1}, \quad (5.16)$$

where  $j'_{m,1}$  and  $j_{m,1}$  are the first zeroes of  $J'_m$  and  $J_m$  respectively.

Furthermore, since

$$\frac{J_m(b_m)}{b_m J'_m(b_m)} \leq \frac{J_m(b_m^{(0)})}{b_m^{(0)} J'_m(b_m^{(0)})},$$

where  $b_m^{(0)} = (b_m)_{\Omega^2=0}$ , instability occurs if the following condition is satisfied:

$$\frac{J_m(b_m^{(0)})}{b_m^{(0)} J'_m(b_m^{(0)})} \geq -\frac{K_{\parallel}^2}{m^2 M^2} \frac{1}{m^2 + 1}. \quad (5.17)$$

We can determine  $K_{\parallel}$  corresponding to marginal stability. From (5.9), we have

$$K_{\parallel} = \frac{2mM^3}{b_m^{(0)2}} \pm \sqrt{\frac{4M^2m^2}{b_m^{(0)2}}(M^4/b_m^{(0)2} - \Pi)}. \quad (5.18)$$

Substituting for  $K_{\parallel}$  in (5.17), we finally have the condition for instability as

$$\begin{aligned} \frac{J_m(b_m^{(0)})}{b_m^{(0)}J'_m(b_m^{(0)})} &\geq \frac{-4}{(m^2+1)b_m^{(0)2}} \times \\ &\times \left[ \frac{M^4}{b_m^{(0)2}} + \left( \frac{M^4}{b_m^{(0)2}} - \Pi \right) \pm \sqrt{\frac{4M^4}{b_m^{(0)2}}(M^4/b_m^{(0)2} - \Pi)} \right]. \end{aligned} \quad (5.19a)$$

To find a criterion for instability, it is only necessary to consider the positive sign in (5.19a). Clearly, for  $\Pi < M^4/b_m^{(0)2}$ , it will always be possible to satisfy (5.19a), since for  $b_m^{(0)}$  between  $j'_{m,1}$  and  $j_{m,1}$ ,  $J_m/b_m^{(0)}J'_m$  varies from  $-\infty$  to 0. The range of  $K_{\parallel}$  for which instability occurs can be found by solving (5.19a) with the equality sign. Let  $b_{m,2}^{(0)}$  and  $b_{m,1}^{(0)}$  denote the solutions for the positive and negative signs respectively ( $b_{m,2}^{(0)} > b_{m,1}^{(0)}$ ). Then the corresponding values of  $K_{\parallel}$  from (5.18) for  $\pi \ll M^4/b_m^{(0)2}$  (i.e. very small pressure gradient) are

$$K_{\parallel,2} = \frac{4mM^3}{b_{m,2}^{(0)2}} - \Pi \quad (5.19b)$$

and

$$K_{\parallel,1} = \Pi \quad (5.19c)$$

respectively, where  $b_{m,2}^{(0)}$  and  $b_{m,1}^{(0)}$  satisfy

$$\frac{J_m}{b_{m,2}^{(0)}J'_m} = \frac{-\Pi}{(m^2+1)M^4}, \quad (5.20a)$$

$$\frac{J_m}{b_{m,1}^{(0)}J'_m} = \frac{-8}{(m^2+1)b_{m,1}^{(0)2}} \left( \frac{2M^4}{b_{m,1}^{(0)2}} - \Pi \right). \quad (5.20b)$$

For the force-free case ( $\Pi = 0$ ), the unstable domain of wave numbers is given by  $4mM^3/b_{m,1}^{(0)2} > K_{\parallel} > 0$ . The effect of introducing a positive radial pressure gradient ( $\Pi > 0$ ), is to decrease the interval of for which instability occurs. The critical pressure gradient which will stabilize the configuration is given by

$$\Pi_c = M^4/b_{m,c}^{(0)2}. \quad (5.21)$$

For  $\Pi > \Pi_c$  (5.19a) cannot be satisfied, as the right hand side is imaginary, and hence the system is stable. The value of  $b_{m,c}^{(0)}$  can be determined from the equation

$$\frac{J_m}{b_{m,c}^{(0)}J'_m} = \frac{-4M^4}{(m^2+1)b_{m,c}^{(0)4}}. \quad (5.22)$$

It is possible to show from (5.21) and (5.22), that  $\Pi_c$  decreases with increasing  $m$ . Thus if the configuration can be stabilized for the  $m = 1$  mode, it will also be

stabilized for all higher modes, a conclusion that is in agreement with a well known theorem in MHD (Newcomb, 1960).

An approximate value for  $\Pi_c$  can be determined for  $M \ll 1$ , by noting that the right hand side of (5.32) is very small and consequently  $b_{1,c}^{(0)} \approx j_{1,1} = 3.83$ . For  $M = 0.25$ , (5.21) gives  $\Pi_c \approx 2.7 \times 10^{-3}$  which corresponds to a pressure ratio  $p_e/p_0 \approx 1.3$  for  $\beta_0 = 0.05$ . Table I shows the unstable domain of wavenumbers and also the maximum growth rate as a function of  $\Pi$  obtained from (5.9) and (5.15a). This behaviour will be discussed in some detail in the following sections.

TABLE I

The wave-numbers  $K_{\parallel,1}$  and  $K_{\parallel,2}$  corresponding to marginal stability along with the maximum growth-rate are given for different values of the pressure-gradient when  $M = 0.025$ .  $K_{\parallel,max}$  is the wave-number at which the growth-rate attains a maximum value. Note that the range of unstable wave-numbers is independent of  $\beta_0$ . A dash is used when there is no instability

$\Pi$	$K_{\parallel,1}$	$K_{\parallel,max}$	$K_{\parallel,2}$	$-\Omega^2 \text{ max}$	
				$\beta_0 = 0.05$	$\beta_0 = 0.5$
0	0	$3.1 \times 10^{-3}$	$4.2 \times 10^{-3}$	$3.4 \times 10^{-8}$	$3.2 \times 10^{-8}$
$9 \times 10^{-5}$	$4 \times 10^{-4}$	$2.9 \times 10^{-3}$	$3.8 \times 10^{-3}$	$2.0 \times 10^{-8}$	$1.9 \times 10^{-8}$
$18 \times 10^{-5}$	$9 \times 10^{-4}$	$2.6 \times 10^{-3}$	$3.3 \times 10^{-3}$	$8 \times 10^{-8}$	$8 \times 10^{-8}$
$27 \times 10^{-5}$	-	-	-	-	-

5.2. MODERATE TO LARGE  $M$

We shall now solve the eigen-value problem for the growth rates in the most general case. Equations (5.2), (5.7) along with the condition  $r\xi_r = 0$  at  $r = 0$  will be used to determine  $\Omega^2$ . Owing to the complexity of the equations, a numerical solution will be attempted. The wave-numbers corresponding to marginal stability will also be found. In the latter case, (5.2) simplifies to (for  $K_{\parallel} \neq 0$ )

$$\frac{d}{du} \left( \frac{K_{\parallel}^2 B_z^2}{m^2 + K^2 u^2} \frac{d\chi}{du} \right) - \frac{1}{u} \left[ K_{\parallel}^2 B_z^2 + \left( 2B_{\theta}^2 / u B^2 - \frac{4mB_{\theta}B_zK_{\parallel}}{(m^2 + K^2 u^2)B^2} \right) \times \right. \\ \left. \times \frac{dp}{du} - \frac{4k^2 m B_{\theta} B_z K_{\parallel} u}{(m^2 + K^2 u^2)^2} - \frac{4B_{\theta}^2 B_z^2 K_{\parallel}^2}{(m^2 + K^2 u^2)B^2} \right] \chi = 0. \tag{5.23}$$

For  $K_{\parallel} \approx 0$  the exact equation must be used. It is worth observing from (5.23) that the wave-numbers which demarcate the region of instability are independent of the effects of compressibility and also of  $\beta_0$ . However, this is not true for the growth rates of the unstable modes.

Thus if the sole aim is to determine the range of wavenumbers for which instability occurs, one can simply consider (5.2) and (5.3) in the incompressible limit (i.e.  $\gamma \rightarrow \infty$ ), though the frequency spectrum obtained by this method will obviously be

different from the true one. Since we are also interested in finding the growth rates, this limit will not be taken.

## 6. Results

Let us now look at the results of the calculations, which were carried out using standard numerical algorithms.

TABLE II

The wave-numbers  $K_{\parallel,1}$  and  $K_{\parallel,2}$  for which marginal stability occurs, the maximum growth rate  $-\Omega_{\max}^2$  and the pressure ratio  $p_e/p_0$  are shown for different values of  $M$  and  $E$  for  $\beta_0 = 0.05$

$M$	$E$	$K_{\parallel,1}$	$K_{\parallel,2}$	$-\Omega_{\max}^2$	$p_e/p_0$
1.0	1.00	0	0.22	$1.5 \times 10^{-3}$	6.0
	1.02	0.05	0.18	$0.2 \times 10^{-3}$	6.4
	1.04	—	—	—	6.8
1.5	1.50	0	0.59	$1.1 \times 10^{-2}$	5.2
	1.60	0.27	0.42	$0.2 \times 10^{-3}$	6.8
	1.61	—	—	—	6.9
2.0	2.00	0	1.10	$3.1 \times 10^{-2}$	4.2
	2.21	0.52	0.84	$0.6 \times 10^{-3}$	6.8
	2.23	—	—	—	7.1
2.5	2.5	0	1.8	$5.4 \times 10^{-2}$	3.4
	2.8	0.7	1.5	$0.3 \times 10^{-2}$	6.6
	3.0	—	—	—	8.3
3.5	3.5	0	3.2	$1.1 \times 10^{-1}$	2.4
	4.0	1.0	2.8	$0.9 \times 10^{-2}$	6.5
	4.5	—	—	—	9.4
5.0	5.0	0	5.4	$2.3 \times 10^{-1}$	1.7
	6.0	1.9	5.2	$4 \times 10^{-5}$	7.5
	7.5	4.9	5.1	$2 \times 10^{-5}$	12.3

Table II shows the wave-numbers corresponding to marginal stability for different  $M$  and  $E$ . Instability occurs for  $K_{\parallel,1} < K_{\parallel} < K_{\parallel,2}$ . The case  $E = M$ , of course, corresponds to the force-free field i.e. no pressure gradient. The stabilizing effect of a positive pressure gradient (i.e.  $E > M$ ) can be seen quite clearly. For a fixed value of  $M$ , as  $E$  increases, we see as before, that the range of wave-numbers in which instability occurs shrinks and for  $M$  large enough it disappears altogether for small to moderate  $M$  ( $M < 5$ ). However, if  $M$  becomes too large ( $M \geq 5$ ), no matter how large the pressure gradient, instability still persists in a narrow band close to  $K = 0$ . It is worth pointing out that the range of unstable wave-numbers is altered if different boundary conditions are used, as a comparison with an earlier paper (Hasan, 1978) shows, where a rigid boundary was assumed.

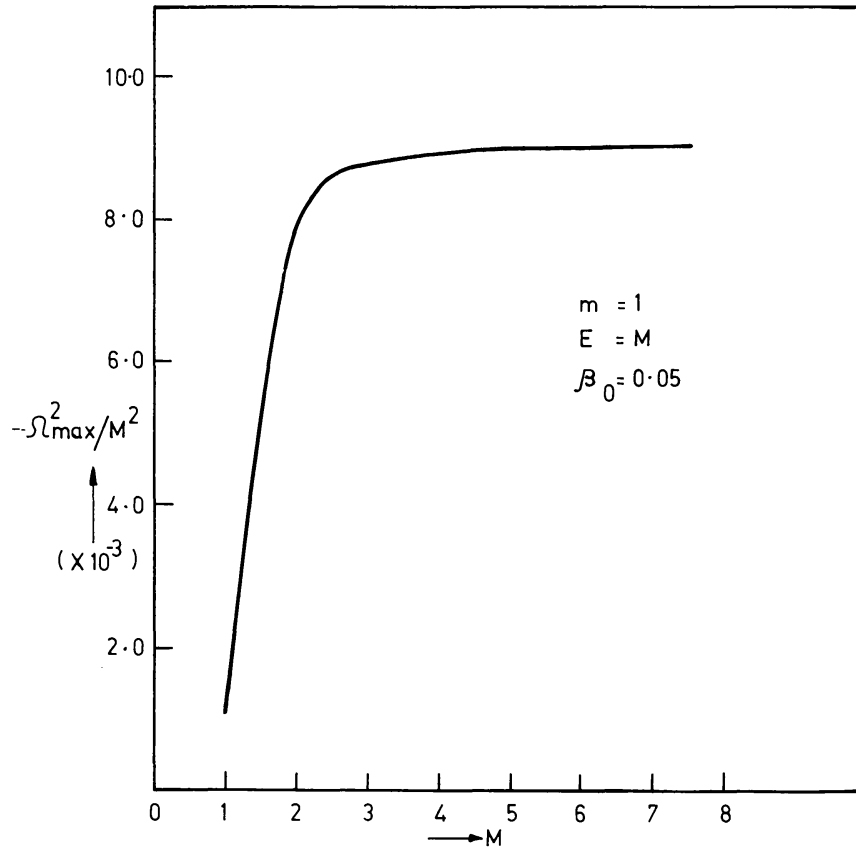


Fig. 2. The behaviour of  $-\Omega_{\max}^2/M^2$  as a function of  $M$  is illustrated for the kink mode in the force-free case.

Figure 2 depicts the dispersion curves of the kink mode for both force-free and non-force-free cases. We can see the marked reduction in the growth-rates brought about by the introduction of a small positive pressure gradient. In Figure 3, the maximum growth rate is shown as a function of  $M$  for the force-free case. For  $M \geq 1$ ,  $-\Omega_{\max}^2/M^2$  increases very rapidly, but for higher values it shows a tendency to level off.

So far the discussion has centered on the  $m = 1$  or kink mode because it is the most difficult to stabilize. We can notice this from Table III in which  $K_{\parallel,1}$  and  $K_{\parallel,2}$  are given for the  $m = 0, 1$ , and  $2$  modes, respectively. It may be observed that the  $m = 0$  or 'sausage' mode is stable even in the force-free case. The  $m = 2$  mode is unstable over a smaller domain of wave-numbers than the kink mode. Furthermore, the pressure gradient required to stabilize it is also less than for the kink mode.

## 7. Discussion

In the preceding sections, the equilibrium and stability of a configuration, which may be related to a pre-flare loop, was studied. Stability was examined mainly with respect to the kink mode, which we found to be the most unstable. The reason for this is that the kink is a practically incompressible mode and requires minimal energy to

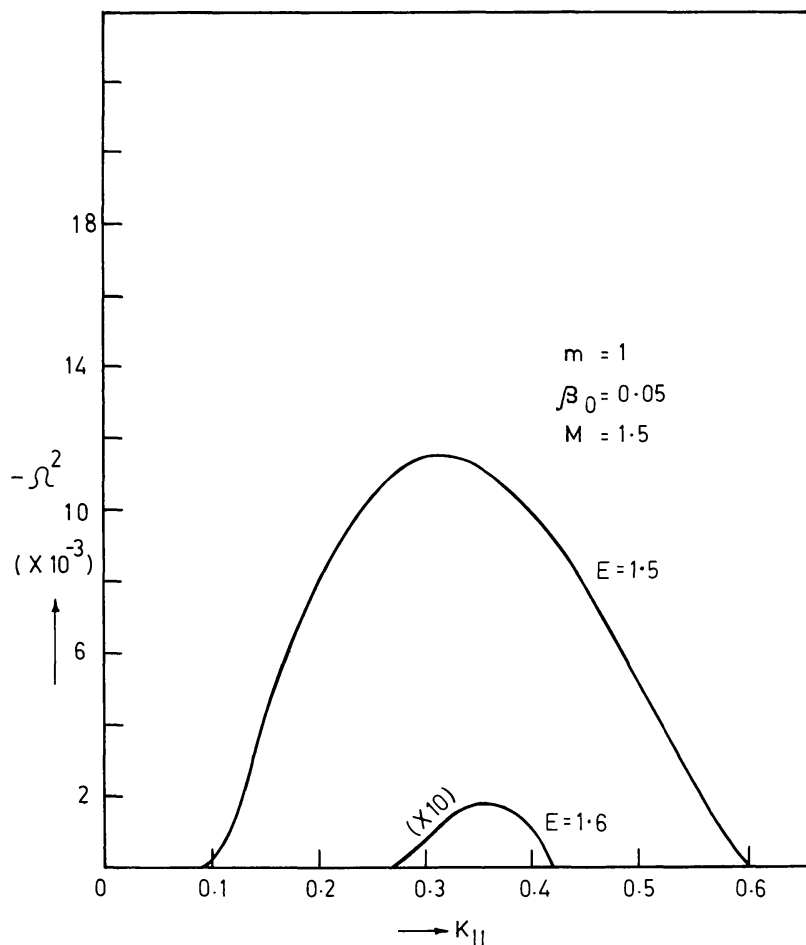


Fig. 3. The dispersion curves depicting the growth rate  $-\Omega^2$  as a function of wave-number  $K_{||}$  are shown for the kink mode both in the absence of and in the presence of a positive radial pressure gradient.

TABLE III

The unstable domain of wave-numbers for different values of the mode-number  $m$  for  $M = 1.5$ . The symbol  $S$  means that the mode is stable

$E$	$K_{  ,1}$			$K_{  ,2}$		
	$m=0$	1	2	0	1	2
1.50	$S$	0	0	$S$	0.59	0.45
1.52	$S$	0.06	0.1	$S$	0.57	0.39

be excited as opposed to other modes which are compressible. Physically, the kink instability is driven by the force exerted by the azimuthal field and results in a global screw-like deformation of the configuration. The tendency to kink is opposed by the longitudinal field inside the flux-tube, which therefore, provides a stabilizing influence.

Let us now examine the results of the stability calculations. We see that the force-free configuration, when the field has a constant pitch, is always unstable. This

result is in agreement with the conclusion reached by Anzer (1968) who studied a class of force-free configurations possessing cylindrical symmetry. The linear growth time  $\tau$  for the kink instability is given by

$$\tau = \frac{a^3 \sqrt{\rho \mu_0} \ln(1 + E^2)}{\pi F} \frac{1}{E^2} \frac{1}{(-\Omega^2)^{1/2}}. \quad (7.1)$$

Choosing  $a \approx 2000$  km,  $F \approx 3 \times 10^{10}$  Wb,  $\rho \approx 1.6 \times 10^{-10}$  kg m<sup>-3</sup> we get

$$\tau \approx \frac{\ln(1 + E^2)}{E^2} \frac{1}{(-\Omega^2)^{1/2}}.$$

For  $M = E = 1.5$ , we find from Figure 3,  $-\Omega_{\max}^2 = 0.012$  and hence

$$\tau \approx 6 \text{ s},$$

which is a very small time indeed compared to the duration of the PFP, which is likely to be several hours.

We shall now discuss the effect on stability of a positive radial pressure gradient within a loop. As seen in the preceding section this has a definite stabilizing influence, a result which has also been obtained earlier by Van Hoven *et al.* (1977) (see also Giachetti *et al.*, 1977), though for a different equilibrium configuration. It is, however, worthwhile pointing out here that for a magnetic structure, characterized by the twist parameter  $M$ , the pressure gradient required for stability must not be too large as an increase in the pressure gradient also results in a reduction of the magnetic energy (see Equations (4.10) and (4.11)) and consequently a larger value for  $M$  would be required to obtain the same energy as before. However, as was mentioned earlier,  $M$  should not become too large, otherwise the configuration is always unstable (see Table II). In a typical situation, for a configuration possessing adequate energy for a small flare, the twist parameter  $M$  could be about 1.5 and the critical pressure gradient needed for stability would require  $E \approx 1.6$  (see Table II). The critical pressure distribution for  $\beta_0 = 0.05$  is shown in Figure 4.

We shall now estimate the magnitude of the critical pressure gradient for a pre-flare loop. Using Equation (4.9), it is easily seen that the ratio of the pressure just outside the loop to the pressure on its axis is

$$p_e/p_0 \approx 6. \quad (7.2)$$

For a magnetic field on the axis  $B_0 \approx 0.005$  Wb m<sup>-2</sup> and  $\beta_0 \approx 0.05$ , we get  $p_0 \approx 0.5$  N m<sup>-2</sup>. Taking a plasma density on the axis  $n_0 \approx 10^{17}$  particles m<sup>-3</sup> which is consistent with observations of flare regions at a height  $\approx 10^4$  km (Jordan, 1976), we obtain a temperature on the axis  $T_0 \approx 5 \times 10^5$  K. Assuming that the plasma density is practically constant radially so that  $n_0 \approx n_e$ , we find from (7.2),  $T_e \approx 3 \times 10^6$  K, which does not conflict with observations of temperatures in flare regions.

We thus find that the pressure gradients required for stability are at least consistent with observations. At present observations of pre-flare loops are inadequate to decide whether such pressure gradients actually exist. For coronal loops, however,

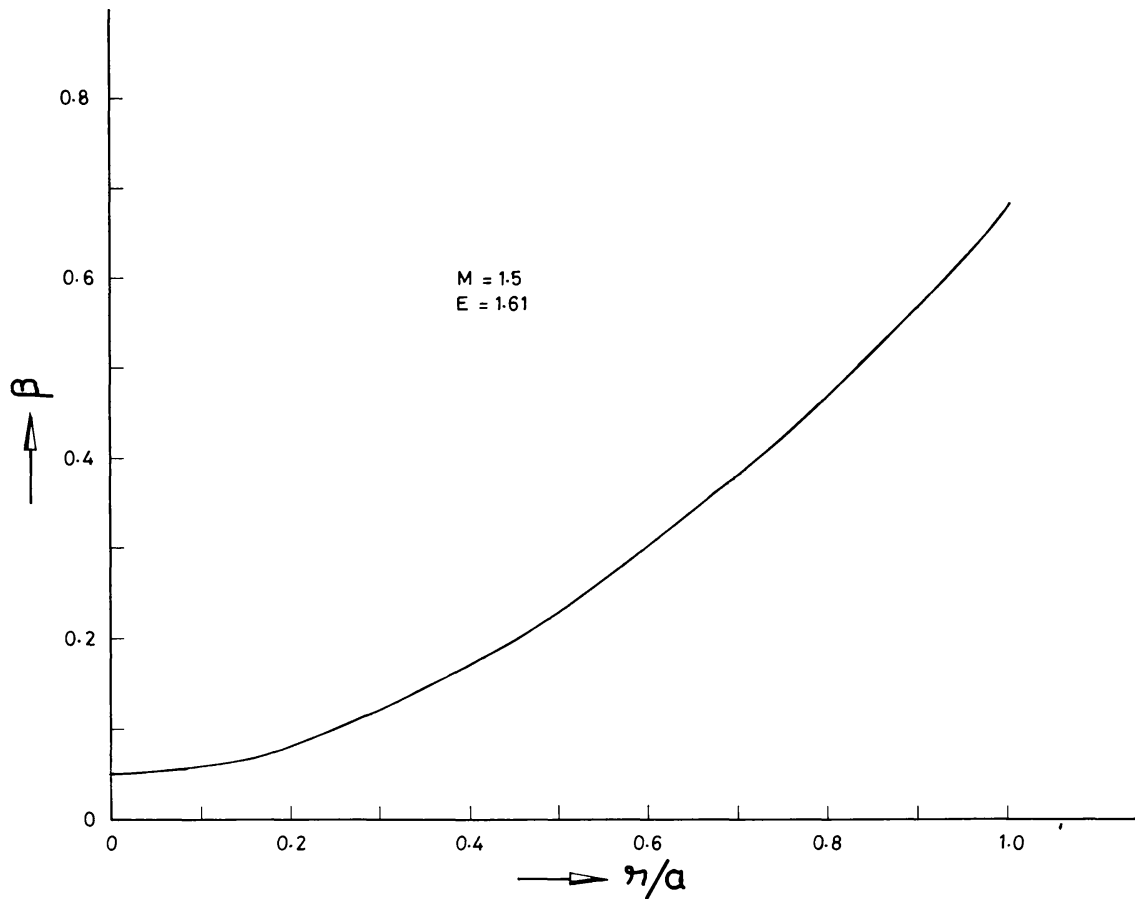


Fig. 4. The variation of  $\beta$  with  $r/a$  is shown for a typical case when the pressure gradient is just sufficient to produce a stable configuration.

Foukal (1975, 1976) has found temperature depressions on the axis varying from one to two orders of magnitude. Thus, if such pressure gradients can also exist in pre-flare-loops, then it is possible to have a stable configuration of the type studied in this paper.

Lastly, let us qualitatively examine the effects of line-tying on stability. If the ends of the loop are anchored firmly, so that they do not suffer any displacement, then the maximum wavelength of the perturbations that can be excited is roughly given by  $\lambda_{\max} \approx L$ . Thus a condition for stability can be expressed as  $\lambda \geq L$  or  $|K| < 2a/R$  (assuming a semi-circular loop) where  $K = 2\pi a/\lambda$ . Since  $|K_{\max}| \approx M$  for a force-free field, the aspect ratio  $R/a$  should be smaller than  $2/M$ . For  $M \approx 1$ , we must have  $R/a \leq 2$ , a condition which is unlikely to hold for flare loops, as from observations we know that the aspect ratio is much larger than unity. If we take  $R/a \approx \frac{1}{8}$ , then the condition for stability becomes  $M \leq 0.25$  or  $N \leq 1$ , where  $N$  is the number of turns a field line makes over the length of the loop. Thus line-tying alone can stabilize only those force-free configurations where the field has a large pitch (roughly when the field makes less than 1 total turn), but not flare loops.



## 8. Conclusions

The purpose of this study was to demonstrate that a stable configuration is possible for a loop in which adequate magnetic energy can be stored prior to the flare. It was shown that a cylindrically symmetric force-free field with a constant pitch is unsuitable as it is unstable for any degree of twist. However, we found that the constant pitch field in the presence of a small transverse pressure gradient can be stable and hence provide an acceptable configuration for energy storage.

## Acknowledgements

I have benefited greatly from several useful discussions at the IAU Colloquium on solar prominences held at Oslo in 1978. I am especially grateful to Drs D. ter Haar and M. H. Gokhale for reading the manuscript and providing helpful suggestions. The computing facilities of the Indian Institute of Science are also thankfully acknowledged.

## References

- Alfvén, H. and Carlquist, P.: 1967, *Solar Phys.* **1**, 220.  
 Altschuler, M. D.: 1974, in G. Newkirk, Jr. (ed.), 'Coronal Disturbances', *IAU Symp.* **57**, 3.  
 Anzer, U.: 1968, *Solar Phys.* **3**, 298.  
 Bernstein, I. B., Frieman, E. A., Kruskal, M. D., and Kulsrud, R. M.: 1958, *Proc. Roy. Soc.* **A244**, 17.  
 Brueckner, G. E., Patterson, N. P., and Scherrer, V. E.: 1976, *Solar Phys.* **47**, 127.  
 Cheng, C. C. and Widing, K.: 1975, *Astrophys. J.* **201**, 735.  
 Foukal, P. V.: 1975, *Solar Phys.* **43**, 327.  
 Foukal, P. V.: 1976, *Astrophys. J.* **210**, 575.  
 Giachetti, R., Van Hoven, G., and Chiuderi, C.: 1977, *Solar Phys.* **55**, 371.  
 Goedbloed, J. P. and Hagebuk, E. J.: 1972, *Phys. Fluids* **15**, 1090.  
 Harvey, K. O. and Harvey, J. W.: 1973, *Solar Phys.* **28**, 61.  
 Hasan, S. S.: 1977, unpublished D. Phil. thesis, Oxford.  
 Hasan, S. S.: 1978, *IAU Colloq.* **44**, 233.  
 Jordan, C.: 1976, *Phil. Trans. Roy. Soc. London* **A281**, 391.  
 Kahler, S. W., Krieger, A. S., and Vaina, G. S.: 1975, *Astrophys. J. Letters* **199**, L57.  
 Krall, A. N. and Trivelpiece, A. W.: 1973, *Principles of Plasma Physics*, McGraw-Hill, pp. 241–246.  
 Livingston, W. and Harvey, J. W.: 1969, *Solar Phys.* **10**, 294.  
 Lundquist, S.: 1950, *Ark. Fys.* **2**, 361.  
 Lust, R. and Hain, K.: 1958, *Z. Naturforsch.* **13a**, 936.  
 Moreton, G. and Severny, A. B.: 1968, *Solar Phys.* **3**, 282.  
 Pallavicini, R., Serio, S., and Vaiana, G. S.: 1977, *Astrophys. J.* **216**, 108.  
 Petrasso, R. D., Kahler, S. W., Krieger, A. S., Silk, J. K., and Vaiana, G. S.: 1975, *Astrophys. J. Letters* **199**, L127.  
 Rust, D. M. and Bar, V.: 1973, *Solar Phys.* **33**, 445.  
 Severny, A. B.: 1965, *Astron. Zh.* **42**, 217.  
 Spicer, D. B.: 1977, NRL Report 8036.  
 Van Hoven, G., Chiuderi, C., and Giachetti, R.: 1977, *Astrophys. J.* **213**, 869.  
 Vorpahl, J. A., Gibson, E. G., Landecker, P. B., McKenzie, D. L., and Underwood, J. H.: 1975, *Solar Phys.* **45**, 199.